Molecular and Cellular Endocrinology 596 (2025) 112414

Contents lists available at ScienceDirect

Molecular and Cellular Endocrinology

journal homepage: www.elsevier.com/locate/mce

Estrogen-mediated inhibition of purine metabolism and cell cycle arrest as a novel therapeutic approach in colorectal cancer

Batoul Abi Zamer [a,b], Jasmin Shafarin [b], BasmaM. Sharaf [b], HamzaM. Al Hroub [b], Nelson C. Soares [b,c], Mohammad H. Semreen [b,d], Mawieh Hamad [b,e], Jibran Sualeh Muhammad [a,b,f,*]

[a] Department of Basic Medical Sciences, College of Medicine, University of Sharjah, Sharjah, United Arab Emirates
[b] Research Institute of Medical and Health Sciences, University of Sharjah, United Arab Emirates
[c] Department of Human Genetics, National Institute of Health Doutor Ricardo Jorge (INSA), 1649-016, Lisbon, Portugal
[d] Department of Medicinal Chemistry, College of Pharmacy, University of Sharjah, United Arab Emirates
[e] Department of Medical Laboratory Sciences, College of Health Sciences, University of Sharjah, United Arab Emirates
[f] Department of Biomedical Sciences, College of Medicine and Health, University of Birmingham, Birmingham, United Kingdom

ARTICLE INFO

Keywords:
Colorectal cancer
Estrogen
Purine metabolism
Metabolomics
Transcriptomics

ABSTRACT

Purine metabolism is upregulated in various cancers including colorectal cancer (CRC). While previous work has elucidated the role of estrogen (E2) in metabolic reprogramming and ATP production, the effect of E2 on purine metabolism remains largely unknown. Herein, the impact of E2 signalling on purine metabolism in CRC cells was investigated using metabolome and transcriptome profiling of cell extracts derived from E2-treated HCT-116 cells with intact or silenced estrogen receptor alpha (ERα). Purine metabolic pathway enrichment analysis showed that 27 genes in the *de novo* purine synthesis pathway were downregulated in E2-treated CRC cells. Downstream consequences of E2 treatment including the induction of DNA damage, cell cycle arrest, and apoptosis were all shown to be ERα-dependent. These findings demonstrate, for the first time, that E2 exerts a significant anti-growth and survival effect in CRC cells by targeting the purine synthesis pathway in a ERα-dependent manner, meriting further investigation of the therapeutic utility of E2 signalling in CRC.

1. Introduction

Colorectal cancer (CRC) continues to be the third most diagnosed cancer and the second leading cause of cancer-related death worldwide (Xi and Xu, 2021). Studies have shown that hormone therapy associates with decreased CRC-related mortality rates in females (Barzi et al., 2013). The role of estrogen (E2, 17β estradiol) signaling in CRC, though not well delineated, is pleotropic (Sasso et al., 2019) as it exerts both stimulatory and inhibitory effects on cell proliferation and survival (Sasso et al., 2019).

E2 exerts its influence on target cells by binding to either Estrogen receptor α (ERα) or Estrogen receptor β (ERβ). While ERβ showed no significant change following E2 treatment, the expression of ERα significantly increased in E2-treated HCT-116 cells. ERβ is the primary ER found in both healthy and cancerous colon epithelial tissues; ERα is rarely expressed in the colon. The role of ERβ has been examined extensively in the context of CRC and several studies have reported that the expression of ERβ is diminished in colonic tumorigenesis relative to normal tissue. Inhibition of ERβ has been associated with tumor stage and grade along with other features of poor prognosis of CRC. Additionally, ERβ can independently exert anti-proliferative effects by activating pro-apoptotic signaling via the p38/MAPK pathway, even in the absence of ERα (Caiazza et al., 2015). On the other hand, the role of ERα in CRC is complex and not fully understood. Research suggests that ERα can have both tumor-promoting and tumor-suppressing effects, depending on the context and specific molecular pathways involved (Ditonno et al., 2021). It has been shown that E2 treatment leads to decreased expression of ERβ and increased expression of ERα (Caiazza et al., 2015). Conversely, other studies have shown that treating ovariectomized rats with ERβ agonists resulted in increased apoptosis and decreased proliferation in the ileum and colon. Additionally, ERβ agonist treatment decreased the number of small intestinal polyps in both male and female ApcMin/+ mice (Barzi et al., 2013). Overall, the significance of and the mechanism(s) underlying the role of E2 and ERs

* Corresponding author. Department of Biomedical Sciences, College of Medicine and Health, University of Birmingham, Birmingham, B15 2TT, United Kingdom
E-mail address: j.sualehmuhammad@bham.ac.uk (J.S. Muhammad).

https://doi.org/10.1016/j.mce.2024.112414
Received 4 June 2024; Received in revised form 23 September 2024; Accepted 9 November 2024
Available online 13 November 2024

signaling in CRC remains ambiguous.

Although several studies have demonstrated that E2/ERs induces metabolic reprogramming in breast cancer cells, vis-à-vis, promote glucose consumption and lactic acid production (Garrido et al., 2013), whether a similar effect is precipitated in CRC cells remains an area of active investigation. Cancer cells undergo metabolic reprogramming, which enables them to uphold their redox balance while elevating ATP production to satisfy their increased demand for energy (Abi Zamer et al., 2021). Among the many metabolic pathways that contribute to CRC development and progression is purine metabolism, a complex metabolic pathway that is involved in the synthesis and breakdown of the nitrogenous bases as the building blocks of DNA and RNA. The purine metabolism pathway also contributes to the regulation of energy metabolism and signal transduction (Maiuolo et al., 2016). Balanced purine levels are vital for the growth, proliferation, and survival of all cells. Under physiological conditions, measured expression of purine metabolism-related enzymes and regulatory proteins helps in maintaining the balance between purine synthesis and degradation (Maiuolo et al., 2016). Interestingly, cancer cells have been associated with elevated concentrations of purine metabolites, indicating a disruption in the usual purine balance in such cells (Yin et al., 2018a). Moreover, the activity of several *de novo* purine biosynthetic enzymes are typically upregulated in many cancers including those of the lung, liver, bladder, prostate, colon, endometrium, and breast (De Vitto et al., 2021).

Disrupted expression and/or activity in several purine pathway-related enzymes has emerged as significant contributor to CRC progression (Amir Hashim et al., 2020). Additionally, purine metabolite levels were shown to be elevated in CRC, given their critical function in supplying cells with indispensable energy, cofactors, and DNA/RNA building blocks (ATP and GTP), thus supporting cell survival and growth (Pedley and Benkovic, 2017). Inadequate nucleotide supply during DNA replication may hinder the pace of cell replication, ultimately leading to DNA damage and cell cycle arrest (Yin et al., 2018b). Indeed, the role of purine synthesis in CRC has been established, but there is a scarcity of evidence regarding strategies to address this pathway. In this study we aimed at investigating the impact of E2/ERα signaling on purine metabolism in CRC cells.

2. Methods

2.1. Cell lines and treatments

HCT-116 cells were cultured using a complete RPMI-1640 medium (Sigma-Aldrich, St. Louis, MO, USA), supplemented with 2 mM L-glutamine, 1% non-essential amino acids, 100 U/mL penicillin, 100 μg/mL streptomycin, and 10% fetal bovine serum. Depending on each experimental run, HCT-116 cells were seeded and incubated at 37 °C in a 5% CO_2 environment for 24 h. Following this, 20 nM 17-β-estradiol (E2), 1,3,5-tris (4-hydroxyphenyl)-4-propyl-1H-pyrazole (PPT) at 1 μM, an ERα selective agonist with 410-fold selectivity for ERα (Tocris, Bio-Techne, UK), diluted in 70% ethanol, (Sigma-Aldrich, St. Louis, MO, USA), was introduced to the cells for 48 h. Cells designated as control received the same volume of 70% ethanol, serving as the vehicle.

2.2. RNA interference and gene knockdown

To knockdown *ESR1*, specific small interfering RNA (siRNA) (*ESR1* CAT# 's4824) was acquired from Thermo-Fisher Scientific (Waltham, MA, USA). First, HCT-116 cells were seeded in antibiotic-free media for 24 h. When the cells reached 30–70% confluency they were used for transfection. For the transfection process, we utilized Lipofectamine RNAiMAX Transfection Reagent and Opti-MEM Reduced Serum Medium from Life Technologies. In addition, a negative control, known as siControl, was incorporated. This control comprised stealth RNAi (Life Technologies). Following a 48-h incubation period post-transfection, the cells underwent the required experiments.

2.3. Measurement of full metabolome by LC-MS/MS

A) Materials and Methods materials-methods

Formic acid (FA) was obtained from Fisher Chemical (Geel, Belgium, UK). Methanol (≥99.9 %), acetonitrile and deionized Water, LC-MS CHROMASOLV were purchased from Honeywell (Wunstorfer Strasse, Seelze, Germany). Pierce protease inhibitor cocktail tablets and lysis buffer were purchased from Thermo Scientific (Rockford, USA).

To assess the intracellular metabolites, whole metabolites levels were measured after proper treatment. In brief, 1.0×10^6 of HCT-116 cells were collected and cell extracts were washed twice with 5% of mannitol. The pellet was lysed using 400 μL of protease inhibitor dissolved in lysis buffer, allowing it to sit for 10 min at room temperature. Subsequently, all samples underwent 30 s of vortexing and were sonicated using either the COPLEY sonicator or QSONICA SONICATOR (Qsonica, Newtown, CT, USA) at 30% AMP for 30 s until the pellets dissolved. The resulting solution was transferred to new Eppendorf tubes and centrifuged at 14000 rpm for 5 min. After centrifugation, the supernatant layer was carefully moved to another Eppendorf tube, to which 400 μL of methanol and 300 μL of chloroform were added. Each mixture was vortexed for 30 s and then centrifuged at 14000 rpm for 5 min. The upper layer was transferred and stored in a glass vial. For washing, 300 μL of methanol was added to the white disk and lower layer, vortexed until the white disk broke and settled at the bottom of the Eppendorf. Subsequently, samples were centrifuged at 14000 rpm for 3 min, and the supernatant was transferred into the same glass vial. To dry the solvent, the samples were processed in the EZ-2 Plus (GeneVac, Ipswich, UK) at 37 ± 1 °C. The dried samples were resuspended with 200 μL (0.1% formic acid in deionized water) and vortexed for 2 min for thorough mixing. Finally, the samples were filtered using a hydrophilic nylon syringe filter with a 0.45 μm pore size and returned to the glass insert within LC glass vials for analysis by Q-TOF MS. A quality control (QC) sample was prepared by pooling the same volume (10 μL) from each sample, and all samples were placed in the autosampler at a temperature set at 4 °C.

B) Ultra-High-Performance Liquid Chromatography Coupled to Electrospray Ionization and Quadrupole Time-of-Flight Mass Spectrometry

An ultra-high-performance liquid chromatography system; Elute UHPLC (Bruker Daltonik GmbH, Bremen, Germany) coupled to a quadrupole-time-of-flight mass spectrometer (Q-TOF) was utilized to perform the LC-MS/MS analysis. The system was equipped with an electrospray ionization (ESI) source, a solvent delivery systems pump (Elute UHPLC HPG 1300), an autosampler, and a thermostat column compartment. Windows 10 Enterprise 2016 LTSB was used as the computer operating system. The data management software was Bruker Compass HyStar 5.0 SR1 Patch1 (5.0.37.1), Compass 4.1 for otofSeries, otof Control Version 6.2.

10 μL aliquot of the sample was injected and the separation was performed on a Hamilton® Intensity Solo C18 column (2.1 × 100 mm, 1.8 μm) (Bruker Daltonik) in a column oven temperature set at 35 °C, using solvent A (0.1% formic acid in deionized Water) and solvent B (0.1% formic acid in acetonitrile) with the following gradient elution mode: 0–2 min, 1% B; 2–17 min, 1–99% B; 17–20 min, 99% B; 20–20.1 min, 99–1% B; 20.1–30 min, 1% B. The flow rate was 0.25 mL/min from 0 to 20 min, 0.35 mL/min from 20 min to 28.3 min, and 0.25 mL/min from 28.3 to 30 min.

The ESI source condition for every injection was as follows: The drying gas flow rate was 10.0 L/min at a temp of 220 °C; the capillary voltage was set at 4500 V; the End Plate offset was set at 500 V; the nebulizer pressure of 2.2 bar.

The acquisition involved two segments; auto MS scan, which ranged from 0 to 0.3 min for the calibrant sodium formate, and auto MS/MS

scan with CID acquisition, which included fragmentation and ranged from 0.3 to 30 min. The acquisition in both segments was performed using the positive mode at 12 Hz. The automatic in-run mass scan range was from 50 to 1300 m/z, the width of the precursor ion was ±0.5, the cycle time was 0.5 s, and the threshold was 400 CTS. Active exclusion was excluded after 3 spectra and released after 0.2 min. For MS2 acquisition the data dependent acquisition (DDA) was used, and the collision energy stepping fluctuated between 100 and 250% set at 20 eV.

M/Z measurements were externally calibrated using 10 mM of sodium formate before sample analysis. In addition, sodium formate solution was injected at the beginning of each sample run and used for internal calibration during data processing. TRX-2101/RT-28-calibrants for Bruker T-ReX LC-QTOF (Nova Medical Testing Inc.) was injected before sample analysis to check and test the performance of the column, reversed-phase liquid chromatography (RPLC) separation, multipoint retention time calibration, and the mass spectrometer. Also, TRX-3112-R/MS Certified Human serum for Bruker T-ReX LC-QTOF solution (Nova Medical Testing Inc.) was prepared from pooled human blood and injected before sample analysis to check the performance of the LC-MS instruments.

C) Data Processing and Analysis

The data obtained from the untargeted profiling of metabolites was processed using MetaboScape® 4.0 software (Bruker Daltonics). Bucketing parameters for molecular feature detection of the processed data in T-ReX 2D/3D workflow were as follows: intensity threshold equal to 1000 counts along with minimum peak length of 7 spectra; utilizing peak area for quantifying the feature. Masses were automatically recalibrated using sodium formate within a retention time range between 0 and 0.3 min. The parameters for data bucketing were assigned as follows: Retention time range started at 0.3 min and ended at 25 min, while mass range started at 50 m/z and ended at 1300 m/z, and the MS/MS import method was done using the average spectrum out of all MS/MS spectra. Identification of metabolites was based on mapping the MS/MS spectra and retention time in the HMBD 4.0, an annotated resource designed to satisfy the needs of the metabolomics community. The compounds with MS/MS were identified using library matching through the annotation process. Then, the selected metabolites were filtered by choosing the set with a higher annotation quality score (AQ score) representing the best retention time values, MS/MS score, m/z values, mSigma, and analyte list spectral library. After normalization and imputation, statistical analysis of log10- converted data was performed to determine significant differences in metabolite levels between the comparison groups. The quantification of the data matrix was based on the peak area of each metabolite. The metabolite datasets included only the significant compounds registered in the HMDB 4.0 with ($p < 0.05$).

2.4. Next generation sequencing (NGS)

Total RNA was extracted using RNeasy Mini Kitt (Qiagen, Hilden, Germany) from HCT-116 cells, followed by evaluation of RNA quality and quantity. Then, mRNA molecules were purified from total RNA using oligo(dT) attached magnetic beads and fragmented into small pieces using fragmentation reagent after reaction a certain period in proper temperature. The first strand cDNA was synthesized according to the corresponding procedure on the instrument. Second strand cDNA was prepared using second strand synthesis reaction system (using dUTP instead of dTTP). The sticky ends of the cDNA double stranded were then repaired by reverse transcription and A base was added to the 3′end. After adding linkers to the A base, PCR amplification was performed, and library was validated on the Agilent Technologies 2100 bioanalyzer. The double stranded PCR products were heat denatured and circularized by the splint oligo sequence. The single strand circle DNA (ssCir DNA) were formatted as the final library. The library was amplified with phi29 to make DNA nanoball (DNB) which had more than 300 copies of one molecular. The DNBs were loaded into the patterned nanoarray and single end 50 (pair end 100/150) bases reads were generated in the way of combinatorial Probe Anchor Synthesis (cPAS).

2.5. Cell cycle arrest assay

For cell cycle arrest assay, CRC cells were collected and fixed in 70% ethanol for at least 24 h, then rinsed with cold phosphate-buffered saline (PBS) before being resuspended in a propidium iodide (PI) staining solution containing PI and RNase A. After incubation at room temperature in the dark for 15 min, flow cytometry analysis was performed using a flow cytometer equipped with appropriate filters for PI fluorescence. Data analysis was carried out using FlowJo software to generate DNA histograms, from which cell cycle distributions were determined by examining peak positions and relative peak areas. Unstained control was included for reference.

2.6. Crystal violet staining

CRC cells were plated to achieve 40% confluence and treated with the specified concentration of E2 for a designated time. After treatment, the cells were gently washed with warm PBS and fixed using a citric acid/methanol solution. Subsequently, staining was conducted using a 0.5% crystal violet solution in formalin at room temperature, allowing the stain to interact with the cells for 20–30 min. After staining, the cells were rinsed with tap water and air-dried. For quantitative analysis, the stained cells were dissolved in a 1% sodium dodecyl sulfate (SDS) solution at room temperature, ensuring complete dissolution with proper agitation. The absorbance of the solution was measured at 570 nm using a microplate reader.

2.7. Immunofluorescence staining

Cells were initially fixed with 4% paraformaldehyde for 15 min on shaker at room temperature, permeabilized with 1% Triton X-100, and blocked with a 3% bovine serum albumin (BSA) solution for 1 h. The primary ERα antibody (Ab75635, Abcam, Cambridge, UK) or γH2ax (9718, Cell Signaling Technology) was applied and allowed to incubate overnight at 4 °C, followed by incubation with a fluorophore-conjugated secondary rabbit antibody at room temperature for 2 h. To visualize cell nuclei, DAPI staining was performed for 15 min. After thorough washing with PBS, coverslips were mounted using a suitable mounting medium. Pictures were taken using Olympus Fluorescence Microscope.

2.8. Annexin V and 7-AAD staining

Apoptosis assessment was carried out using Flow Cytometry, which allowed for the detection of phosphatidylserine exposure on the cell membrane surface. After the treatment, the cells were collected using trypsin, and, to ensure cell viability and purity, they underwent three rounds of cold PBS washing to remove any remaining trypsin and cellular debris. A fresh Falcon tube was used to contain 200 μL of the cell suspension, to which Annexin V-FITC (5 μL) and 7-amino actinomycin D (7-AAD) (5 μL) were added. The mixture was gently blended and then incubated in a dark environment at room temperature for 15 min. Subsequently, Flow Cytometry (BD FACS AriaTM III) was employed to analyze apoptosis, following the manufacturer's recommended instructions. To guarantee accuracy, unstained cells and cells single-stained with Annexin V-FITC or 7-AAD controls were used.

2.9. Western blot analysis

To assess protein expression levels, a Western blot analysis method was employed. In this procedure, HCT-116 cells were initially seeded at a concentration of 1×10^6 cells/mL in 60 mm Petri dishes. Then, the cells were exposed to the previously described treatments and left to

incubate for 48 h at 37 °C in a 5% CO2 incubator. Following the specified treatment duration, the CRC cells were harvested and lysed using RIPA buffer, which contained protease and phosphatase inhibitors to maintain protein integrity (Sigma-Aldrich, St. Louis, MO, USA). After quantifying the proteins (Bio-Rad, Hercules, CA, USA), 30–40 μg of protein samples were loaded onto SDS-PAGE gels and subjected to electrophoresis to achieve separation. The separated proteins were then transferred to nitrocellulose membranes. To minimize non-specific binding, the membranes were blocked using a 5% non-fat milk solution in Tris-buffered saline with Tween 20 (TBST). The membranes were subsequently incubated with primary antibodies: CDK-2 (CAT#2546s, Cell Signaling Technology), CDK6 (CAT#Ab151247, Abcam, Cambridge, UK), CDK4 (CAT#Ab68268, Abcam, Cambridge, UK), CyclinD1 (CAT# ab134175, Abcam, Cambridge, UK), Bak (CAT#D2D3, Cell Signaling Technology), Bcl-2 (CAT# ab59348, Abcam, Cambridge, UK) β-actin (CAT#4967s, Cell Signaling Technology) against specific targets overnight at 4 °C. Afterward, the membranes were washed with TBST and incubated with secondary antibodies corresponding to the primary antibodies used. The protein bands were visualized using a chemiluminescence imaging system from Bio-Rad (Hercules, CA, USA).

2.10. Bioinformatics analysis

The evaluation of variations in *ESR1* gene expression between neighboring healthy tissues and tumor tissues in CRC was conducted through the University of Alabama at Birmingham Cancer data analysis Portal (UALCAN) database (http://ualcan.path.uab.edu/). The results with a log-rank p-value of <0.05 were considered significant.

2.11. Statistical analysis

Each experiment was independently replicated three times, and the resulting data was subsequently reported as the mean value along with the standard error. Significance analysis was performed using Student's t-test and a one-way ANOVA test to evaluate the obtained data. Additional statistical calculations were carried out using Microsoft Excel 2010 (Microsoft Office, 2010). The bands derived from Western blots were quantified with ImageLab software, and one representative figure was included. A p-value less than 0.05 was deemed statistically significant.

The metabolite datasets that were exported as a CSV file from Metaboscape were then imported into MetaboAnalyst 5.0 software (Mcgill University, Montreal, QC, Canada), a comprehensive platform for metabolomics data analysis. The sPLS-DA was performed using MetaboAnalyst 5.0 (https://www.metaboanalyst.ca) to select the most discriminative features in the examined group to aid in classifying the samples. The false discovery rate (FDR) method was utilized to correct multiple hypothesis testing and reduce the rate of false positives. The identification of significantly altered metabolites in the E2-treated as opposed to the control group, was accomplished through a two-tailed independent Student's t-test. This led to the creation of a volcano plot, visually representing the statistical significance and fold change ($p < 0.05$, $FC = 1.25$), highlighting the dysregulation of cellular metabolites for each condition. Functional Enrichments were constructed using Metaboanalyst. Additionally, MetaboAnalyst 5.0 was utilized for the enrichment metabolite sets, and pathway analysis. Metabolomics data used in this study are deposited in Metabolomics workbench with (datatrack_id:4483 study_id:ST003029) and the Digital Object Identifier (DOI) for this project (PR001882) is: https://doi.org/10.21228/M8FQ52.

3. Results

3.1. E2 treatment inhibits purine metabolism in HCT-116 cells

The question of whether E2 contributes to metabolic reprogramming in CRC cells was investigated using metabolomic profiling of HCT-116 cells treated with E2 for 24 h. A total of 117 metabolites were measured in control and E2 treated HCT-116 cells (Supplementary Table 1). The heatmap shows the top 50 altered metabolites (Fig. 1). According to the volcano plot, out of the 117 metabolites, 12 have shown significantly different median values between control and treated groups. Of these, 10 were significantly downregulated and 2 were significantly upregulated in E2-treated versus control cells (Fig. 2). Given that E2 is known to have a protective effect against CRC, significantly downregulated metabolites were included in the enrichment analysis of biological process gene ontology terms linked with those metabolites using the Small Molecule Pathway Database (SMPDB)/MetaboAnalyst 5.0 software. This form of analysis showed these metabolites to be more enriched in pathways like purine metabolism, methyl histidine metabolism and sphingolipid metabolism (Fig. 3a). Analysis of drug-related pathways revealed enrichment of mercaptopurine, thioguanine, and azathioprine action pathways (Fig. 3b).

3.2. Purine metabolism is inhibited at the mRNA level in HCT-116 cells

To validate the role of E2 in purine metabolism in HCT-116 cells at the mRNA level, NGS was performed on cell extracts obtained from HCT-116 cells treated with 20 nM E2 for 6 h. Our results showed that around 2600 genes were upregulated, and 2800 genes were downregulated in E2-treated versus control HCT-116 cells (Supplementary Figs. 1S and 2S). The 2600 upregulated genes were found to be enriched in pathways including Protein processing in the endoplasmic reticulum (ER), microRNA in cancer and the Mitogen-Activated Protein Kinase (MAPK) signaling pathway. In contrast, further analysis of the 2800 downregulated genes, purine metabolism pathway was found to be the third most enriched pathway; tricarboxylic acid cycle (TCA) and valine, leucine, and isoleucine degradation were found to be the first and second most enriched pathways (Fig. 4a). 27 genes involved in purine metabolism were significantly downregulated in E2-treated cells. To explore which pathway is mostly targeted by E2 in HCT-116 cells, we used the KEGG database to analyze the exact role of 27 genes in purine metabolism. KEGG analysis showed that these 27 genes were either directly or indirectly involved in the *de novo* purine synthesis pathway (Fig. 4b). To validate these findings, integrated metabolomic and transcriptomic profile analysis was performed using the MetaboAnalyst 5.0 software. This form of analysis revealed an enrichment of the purine metabolism pathway in addition to the pentose phosphate pathway (PPP) and the TCA cycle pathway (Fig. 5) (Supplementary Fig. 3S). This clearly suggests that E2 treatment inhibits the synthesis of purines by targeting the *de novo* purine synthesis pathway in HCT-116 cells.

3.3. The effect of E2 signalling on HCT-1116 metabolism is ERα-dependent

E2 typically exerts its major effects through its binding to ERα (Fuentes and Silveyra, 2019). To examine whether the effects of E2 on purine metabolism in CRC are ERα-dependent, NGS analysis was performed using cell extracts derived from ERα-silenced HCT-116 cells treated with E2. Interestingly, silencing of ERα abolished the observed effects of E2 as described earlier (Fig. 6a). Moreover, 14 out of the 27-purine pathway-related genes that were downregulated in E2-treated cells, were not altered in E2-treated/ERα-silenced cells (Fig. 6b) (Supplementary Fig. 4S). This suggests that E2 requires ERα engagement to mediate its inhibitory effect on purine metabolism in CRC cells.

3.4. E2-ERα complex induces apoptosis and disrupts HCT-116 cell cycle

We initially evaluated the expression of both ERα and ERβ in five distinct CRC cell lines, finding that HCT-116 cells exhibited the highest levels of both ERα and ERβ. Additionally, SW480 displayed the second-highest ERα expression, although its ERβ levels were comparatively

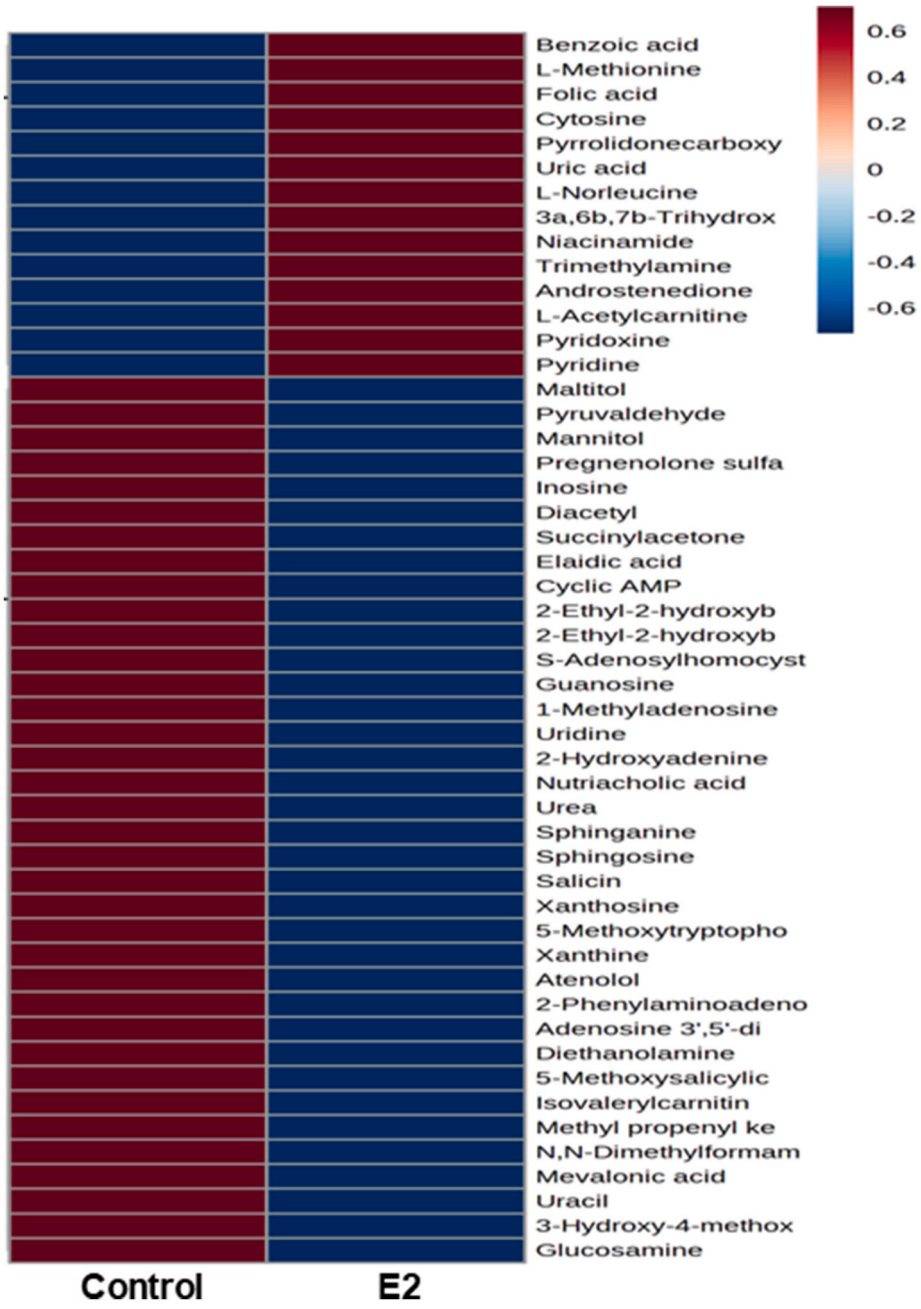

Fig. 1. Metabolomic profiling of HCT-116 cells treated with E2. The heatmap illustrates the top 50 metabolites whose abundance has changed in response to E2 treatment. Upregulated metabolites are indicated in red and downregulated metabolites are depicted in blue.

lower than in the other cell lines (Supplementary Fig. 5S). Previous work has shown that inhibition of purine metabolism is known to inhibit DNA synthesis, mediating cell cycle arrest and halting cell growth (Yin et al., 2018a). We therefore assessed the ability of E2 to induce apoptosis and cell cycle arrest in HCT-116 cells. First, immunofluorescence studies confirmed that E2 treatment increases ERα expression in HCT-116 cells when compared to control or ERα-silenced HCT-116 cells (Fig. 7a). Treatment of HCT-116 and SW480 cells with 20 nM E2 reduced their survival (Fig. 7b) (Supplementary Fig. 6S a-b), and induced apoptosis (Fig. 7c–d) (Supplementary Fig. 6S c-d). Also, the treatment of HCT-116 cells with ERα selective agonist (PPT 1 μM) showed reduced survival and increased apoptotic cell death (Supplementary Fig. 7S a-d). However, ERα-silenced, E2-treated, HCT-116 cells showed no effect on both survival and apoptosis. Expression of the apoptotic protein Bak was significantly increased while that of Bcl-2 was decreased in E2-treated HCT-116 cells (Fig. 7e–f). E2 treatment was also associated with upregulated γH2ax expression, DNA damage, and cell cycle arrest in E2-treated ERα-intact cells, but not E2-treated ERα-silenced cells (Fig. 8a–c). Moreover, HCT-116 cells treated with ERα selective agonist (PPT 1 μM) showed cell cycle arrest (Supplementary Fig. 7S e-f). While the expression of cell cycle markers including Cdk6, Cdk2, and CyclinD1 was inhibited in normal E2-treated HCT-116 cells; it was re-expressed following ERα silencing (Fig. 8d–e).

4. Discussion

The effect of E2 signaling on metabolic reprogramming, in the form of Warburg effect and ATP production, has been previously demonstrated (Hernández-López et al., 2022). However, the impact of E2 signaling on purine metabolism in CRC cells is still under investigation.

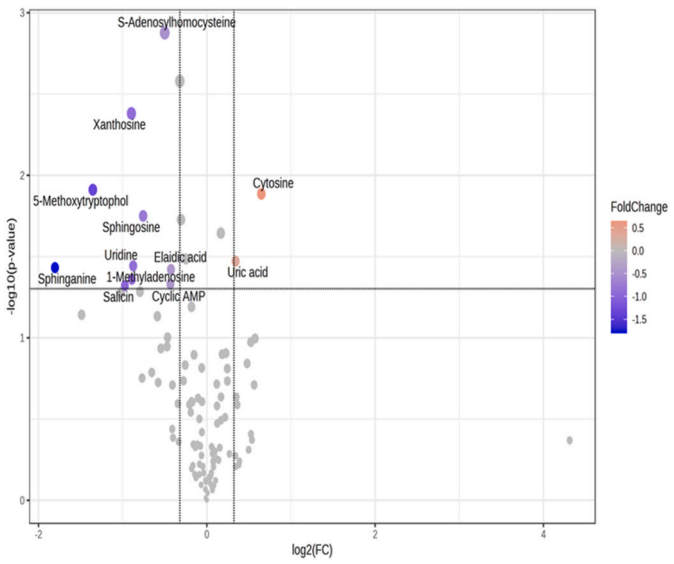

Fig. 2. Volcano plotting of metabolomic profiling of E2-treated HCT-116 cells. The plot highlights metabolites with a 1.25-fold change and statistical significance ($p < 0.05$). X-axis represents the $\log_2$ fold change, indicating the magnitude of change in metabolite abundance between the two conditions and Y-axis represents the negative $\log_{10}$ of the p-value, reflecting the statistical significance of observed changes.

In this study, we showed, for the first time, that E2, by binding to ERα, exerts a significant protective effect against CRC cells through its ability to target and disrupt the purine synthesis pathway. Metabolic profiling, NGS data and integrated OMICs showed an enrichment of purine metabolic pathway. A total of 27 genes involved in do novo purine synthesis pathway were identified to be downregulated in E2-treated CRC cells. Furthermore, E2 treatment upregulated ERα and induced DNA damage, cell cycle arrest and apoptosis in CRC cells; effects which were reversed upon ERα silencing.

The expression of ERs in CRC, specifically ERα and ERβ, plays a significant role in tumour biology. While ERα is often found to be absent or minimally expressed in various CRC cell lines, ERβ shows a more prominent presence (Ditonno et al., 2021). Our results have shown that ERα is expressed in different CRC cell lines and E2 treatment increased ERα expression. In 1999, one study investigated ERs expression in CRC cell lines, finding that while ERα was absent, ERβ was highly expressed in all cell lines. However, in the same study, they conducted binding studies of E2 to these receptors. Their results reported the presence of a high-affinity binding protein in these cells, with binding properties similar to those previously described in various CRC cells and associated with ERα (Fiorelli et al., 1999). However, recent studies have shown that ERβ is often under-regulated in advanced adenomas and CRC, while ERα is more prevalent, and ERβ stimulation has been shown to slow polyp growth and impact CRC pathways, indicating that dietary modulation of ERs could be beneficial, though large-scale clinical trials are lacking (Ditonno et al., 2021). Thus, the debate is still ongoing on the role of ERs and E2 in CRC.

Purine metabolism is divided into three pathways: the *de novo*, the salvage and the degradation pathway. In the purine degradation pathway, uric acid is produced as the final waste product following the breakdown of adenine and guanine. Our metabolic profiling data have shown that uric acid is upregulated in E2-treated CRC cells (Furuhashi, 2020). Studies have shown that hyperuricemia is a marker of the purine degradation pathway (Liu et al., 2021). The fact that sex hormones, including E2 reduce uric acid levels is further of its involvement in the purine synthesis pathway. That said, a recent study has shown that E2 levels positively correlate with uric acid levels in adolescents and adults (Wang and Charchar, 2021). Furthermore, the *de novo* pathway is known to be the fundamental pathway to be upregulated in cancer cell (Yin et al., 2018b; Nishino and Okamoto, 2015). Our results showed that the E2-ERα complex inhibits 27 genes related to the *de novo* purine pathway. On the other hand, other research investigations provide evidence on the carcinogenic role of ERα and its link to Wnt/β-Catenin signaling. In one study, the introduction of ERα into SW480 and HCT116 cells led to the stimulation of Wnt signaling, and the use of an ER antagonist resulted in the inhibition of this pathway. Furthermore, in this same study, the introduction of an antibody against β-Catenin resulted in the activation of the Estrogen Response Element (ERE) in a manner dependent on E2. Furthermore, the protective role of ERβ has already been established in CRC. The introduction of ERβ into CRC cell lines influences the MAPK signaling pathway. Additionally, ERβ leads to the suppression of IL6, thereby diminishing inflammation. Additionally, ERβ is involved in the modulation of the TGFβ signaling pathway in CRC animal model (Barzi et al., 2013). Furthermore, Hiraike et al. found that ERβ plays a crucial role in regulating the colon, as ERβ−/− mice exhibited higher cell proliferation, faster migration towards the luminal surface, decreased apoptosis, and reduced expression of differentiation and adhesion

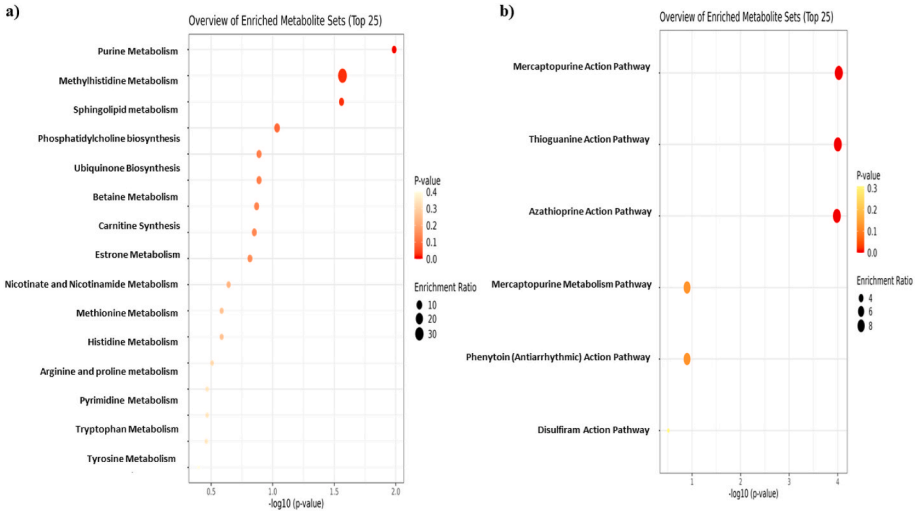

Fig. 3. Enrichment analysis of downregulated metabolites in E2-treated HCT-116. (a) Enrichment analysis of the biological process gene ontology terms linked with obtained metabolites using the Small Molecule Pathway Database (SMPDB) from MetaboAnalyst 5.0 software. (b) Enrichment analysis of Drug-related pathways linked with obtained metabolites using MetaboAnalyst 5.0 software.

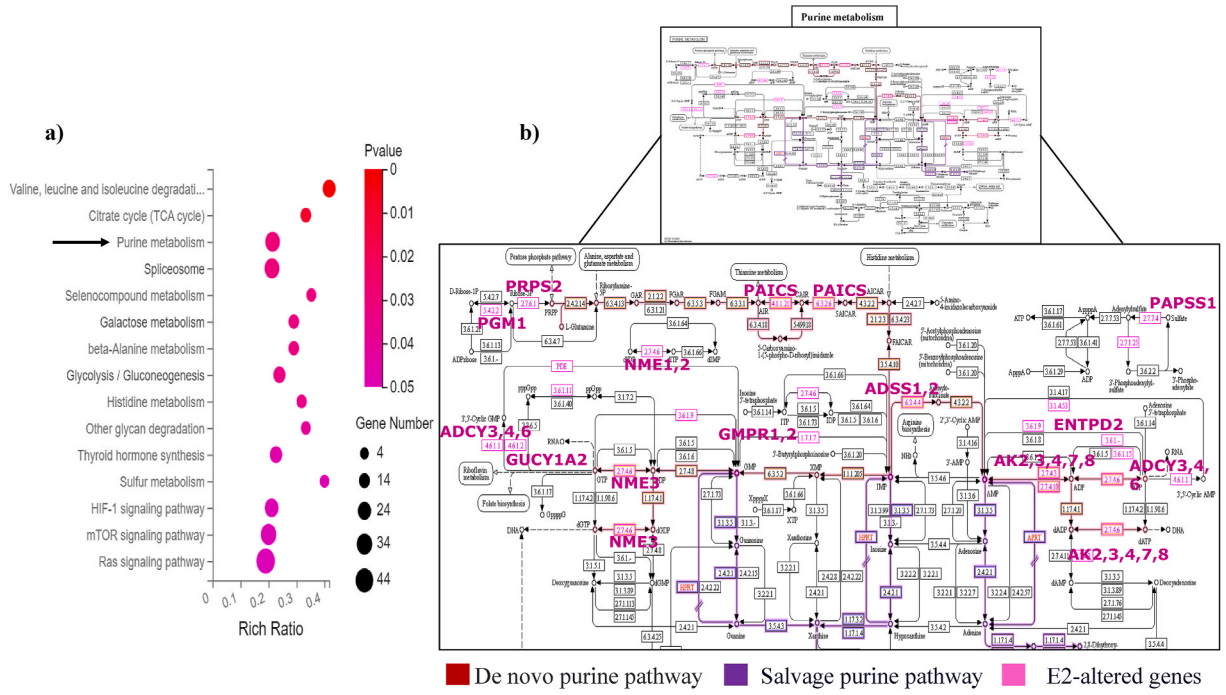

Fig. 4. Transcriptomic analysis of HCT-116 cells treated with E2. (a) Enrichment analysis of the biological processes linked to downregulated genes in HCT-116 treated with E2. (b) A KEGG map representing the function of altered genes in E2-treated cells.

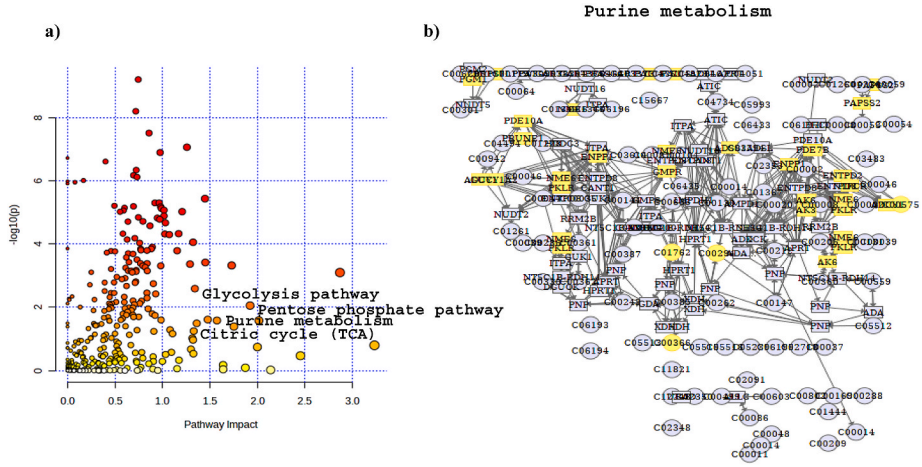

Fig. 5. Integrated analysis of transcriptomics and metabolomics data relating to E2-treated HCT-116 cells. (a) Biological pathways shown to be enriched based on combined transcriptomic and metabolomic data analysis. (b) The chart represents altered genes and metabolites in the purine pathway following E2 treatment.

markers compared to wild-type littermates. These results suggest that ERβ is essential for maintaining the organization and architecture of colonic tissue, preventing the formation of hyperplastic lesions by promoting proper cell shedding (Wada-Hiraike et al., 2006) …

Antimetabolites targeting purine synthesis play a crucial role in treating cancers such as acute lymphocytic leukemia (Ma et al., 2010). Besides, the purine antimetabolites 6-mercaptopurine and azathioprine have been widely used in inflammatory bowel disease (IBD) treatment which are common risk factors for CRC (Nielsen et al., 2001). However, the role of antimetabolites as chemotherapeutics against CRC has yet to be investigated. Our findings demonstrated that E2 reduces the expression of metabolites involved in the action of several antimetabolites including 6-mercaptopurine, thioguanine, and azathioprine. Therefore, we suggest that antimetabolites could be a potential chemotherapy approach for CRC treatment.

Purine synthesis is upregulated to support the heightened demand for nucleotides, facilitating accelerated DNA and RNA synthesis, essential for the uncontrolled proliferation of cancer cell (Yin et al., 2018b). It is well known that cells enhance the synthesis of purine nucleotides either before or during the S-phase of the cell cycle. Besides, a study has shown that the rate of *de novo* purine synthesis exhibited a 5.0-fold increase, during the transition from mid-G1-phase to early S-phase (Fridman et al., 2013). Our findings have shown that the inhibition of purine metabolism by E2 arrested CRC cells at G1 phase. We also reported an induction of apoptosis in E2-treated CRC cells. Inhibition of several enzymes involved in purine metabolism has been shown to induce apoptosis in various cancers including CRC (Camici and Pesi, 2019). In our study, E2 treatment may have influenced purine metabolism in CRC cells, either directly or indirectly, leading to metabolic stress. This stress could sensitize the cells to mitochondrial dysfunction and subsequent activation of the intrinsic apoptosis pathway. The E2-mediated modulation of signaling pathways, such as those involving

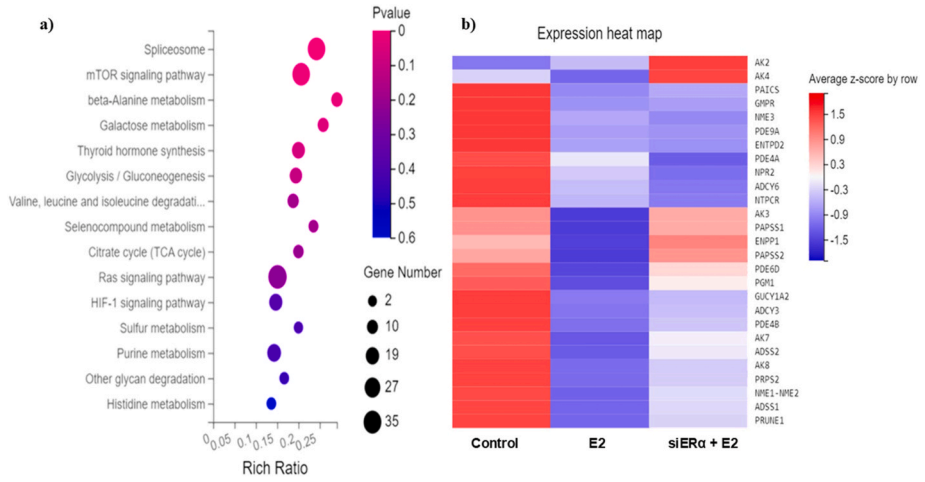

Fig. 6. Role of ERα in E2-induced inhibition of purine metabolism in HCT-116 cells. (a) Enrichment analysis of the biological process linked with downregulated genes in ERα-silenced HCT-116 treated with E2. (b) Expression pattern of the 27 genes enriched in purine metabolism pathway between control, E2-treated and E2-treated/ERα-silenced HCT-116 cells.

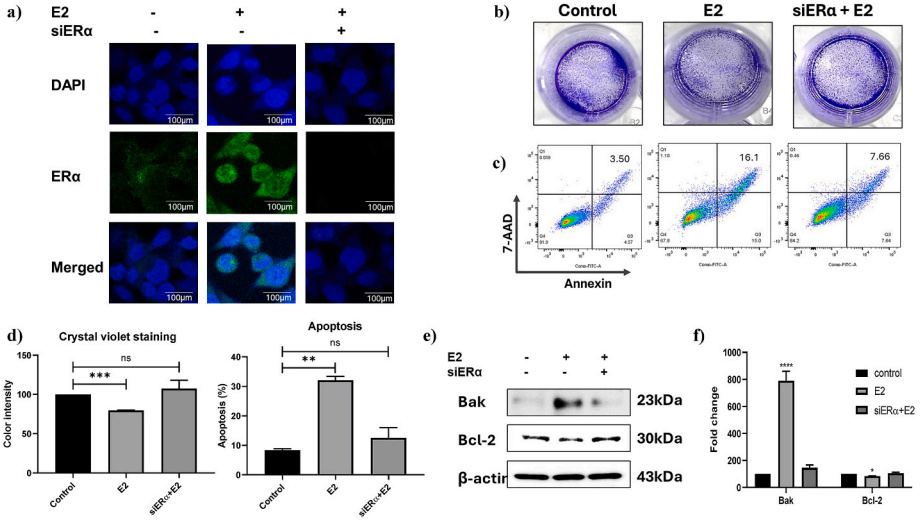

Fig. 7. E2 treatment reduces HCT-116 cell survival. (a) ERα expression and DAPI staining following E2 treatment in ERα-silenced and control cells. (b) Crystal violet staining showing the effect of E2 treatment in ERα-silenced and control HCT-116 cell. (c) Apoptosis was evaluated using Annexin/7-AAD staining following E2 treatment in ERα-silenced and control HCT-116 cells. (d) Quantification of crystal staining and apoptosis. (e) Expression of apoptosis-related proteins in ERα-silenced and control HCT-116 cells following E2 treatment. (f) Quantification of the Western blot bands using Image Lab.

ERα, could also influence the balance between cell survival and apoptosis by affecting mitochondrial integrity and the expression of pro-apoptotic proteins. Both Bak and Bcl-2 are markers of intrinsic apoptosis pathway (Dai et al., 2009). Our findings indicate an upregulation in Bak expression and a concurrent inhibition of Bcl-2 expression, suggesting the activation of the mitochondrial apoptosis pathway. Inhibition of purine metabolism disrupts the DNA and RNA production process, leading to cellular stress and triggering apoptosis, particularly through the mitochondrial (intrinsic) apoptosis pathway. Inhibition of purine metabolism has been reported to induce the mitochondrial apoptosis pathway (Aghaei et al., 2011; Saitoh et al., 2004).

In conclusion, our study unveiled a novel aspect of E2-ERα signaling in CRC cells. While previous work has demonstrated that E2 modulates metabolism and ATP production, the exact impact of E2 signaling on purine metabolism in CRC cells was not well understood. Our findings demonstrated, for the first time, that E2 exerts a significant protective effect against CRC cells through its ability to target and disrupt the purine synthesis pathway in an ERα-dependent manner. These observations call for further examination of the therapeutic utility of E2-ERα signaling in CRC.

CRediT authorship contribution statement

Batoul Abi Zamer: Writing – original draft, Methodology, Investigation, Formal analysis, Data curation, Conceptualization. **Jasmin Shafarin:** Methodology, Data curation. **BasmaM. Sharaf:** Methodology, Data curation. **HamzaM. Al Hroub:** Methodology, Investigation, Data curation. **Nelson C. Soares:** Methodology, Formal analysis. **Mohammad H. Semreen:** Writing – review & editing, Validation, Methodology. **Mawieh Hamad:** Writing – review & editing, Validation. **Jibran Sualeh Muhammad:** Writing – review & editing, Writing – original draft, Validation, Supervision, Resources, Project administration, Funding acquisition, Data curation, Conceptualization.

Informed consent statement

Not applicable.

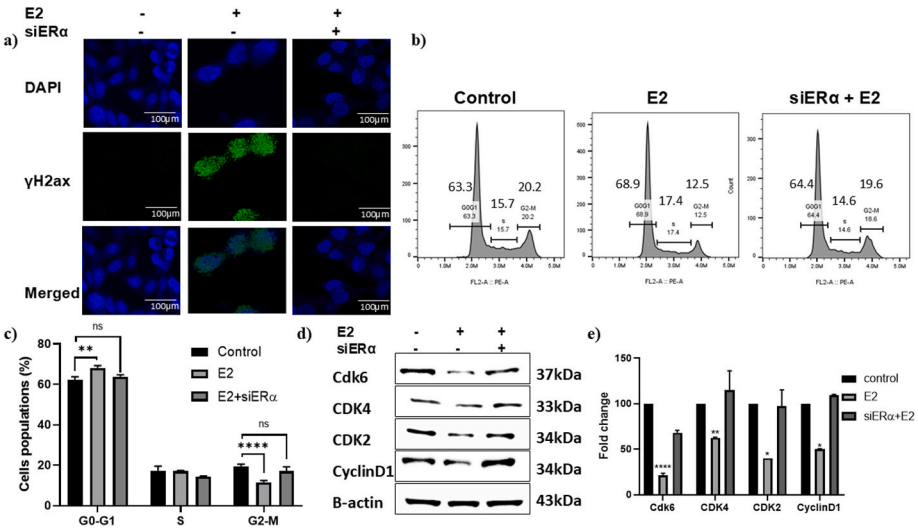

Fig. 8. ERα silencing diminishes the negative effects of E2 treatment CRC cell cycling. (a) γH2ax expression and DAPI staining following E2 treatment in ERα-silenced and control HCT-116 cells. (b) HCT-116 cells were stained with PI to identify G0/G1, S and G2/M phase populations using flow cytometry. (c) Quantification of cell cycle phases. (d) Expression of cell cycle regulatory proteins in ERα-silenced and control HCT-116 cells following E2 treatment. (e) Quantification of the Western blot bands using Image Lab.

Institutional review board statement

Not applicable.

Funding

J.S.M. is funded by the King Hussein Cancer Foundation, Jordan (2022-KHA-001), and the Research Institute of Medical and Health Sciences, University of Sharjah (Project 23010901133).

Declaration of competing interest

The authors declare that they have no known competing financial interests or personal relationships that could have appeared to influence the work reported in this paper.

Acknowledgments

None.

Appendix A. Supplementary data

Supplementary data to this article can be found online at https://doi.org/10.1016/j.mce.2024.112414.

Data availability

The metabolomics data utilized in this study have been deposited in the Metabolomics Workbench under the datatrack_id:4483 and study_id: ST003029. The DOI for this project is https://doi.org/10.21228/M8FQ52 (PR001882).

References

Abi Zamer, B., Abumustafa, W., Hamad, M., Maghazachi, A.A., Muhammad, J.S., 2021. Genetic mutations and non-coding RNA-based epigenetic alterations mediating the Warburg effect in colorectal carcinogenesis. Biology (Basel) 10. https://doi.org/10.3390/biology10090847.

Aghaei, M., Panjehpour, M., Karami-Tehrani, F., Salami, S., 2011. Molecular mechanisms of A3 adenosine receptor-induced G1 cell cycle arrest and apoptosis in androgen-dependent and independent prostate cancer cell lines: involvement of intrinsic pathway. J. Cancer Res. Clin. Oncol. 137, 1511–1523. https://doi.org/10.1007/s00432-011-1031-z.

Amir Hashim, N.A., Ab-Rahim, S., Wan Ngah, W.Z., Nathan, S., Ab Mutalib, N.S., Sagap, I.A., Jamal, A.R., Mazlan, M., 2020. Global metabolomics profiling of colorectal cancer in Malaysian patients. Bioimpacts 11, 33–43. https://doi.org/10.34172/bi.2021.05.

Barzi, A., Lenz, A.M., Labonte, M.J., Lenz, H.-J., 2013. Molecular pathways: estrogen pathway in colorectal cancer. Clin. Cancer Res. 19, 5842–5848. https://doi.org/10.1158/1078-0432.CCR-13-0325.

Caiazza, F., Ryan, E.J., Doherty, G., Winter, D.C., Sheahan, K., 2015. Estrogen receptors and their implications in colorectal carcinogenesis. Front. Oncol. 5, 19. https://doi.org/10.3389/fonc.2015.00019.

Camici, Garcia-Gil, Pesi, Allegrini, 2019. Tozzi purine-metabolising enzymes and apoptosis in cancer. Cancers 11, 1354. https://doi.org/10.3390/cancers11091354.

Dai, H., Meng, X.W., Lee, S.-H., Schneider, P.A., Kaufmann, S.H., 2009. Context-dependent bcl-2/Bak Interactions regulate lymphoid cell apoptosis. J. Biol. Chem. 284, 18311–18322. https://doi.org/10.1074/jbc.M109.004770.

De Vitto, H., Arachchige, D.B., Richardson, B.C., French, J.B., 2021. The intersection of purine and mitochondrial metabolism in cancer. Cells 10. https://doi.org/10.3390/cells10102603.

Ditonno, I., Losurdo, G., Rendina, M., Pricci, M., Girardi, B., Ierardi, E., Di Leo, A., 2021. Estrogen receptors in colorectal cancer: facts, novelties and perspectives. Curr. Oncol. 28, 4256–4263. https://doi.org/10.3390/curroncol28060361.

Fiorelli, G., Picariello, L., Martineti, V., Tonelli, F., Brandi, M.L., 1999. Functional estrogen receptor β in colon cancer cells. Biochem. Biophys. Res. Commun. 261, 521–527. https://doi.org/10.1006/bbrc.1999.1062.

Fridman, A., Saha, A., Chan, A., Casteel, D.E., Pilz, R.B., Boss, G.R., 2013. Cell cycle regulation of purine synthesis by phosphoribosyl pyrophosphate and inorganic phosphate. Biochem. J. 454, 91–99. https://doi.org/10.1042/BJ20130153.

Fuentes, N., Silveyra, P., 2019. Estrogen receptor signaling mechanisms. Adv Protein Chem Struct Biol 116, 135–170. https://doi.org/10.1016/bs.apcsb.2019.01.001.

Furuhashi, M., 2020. New insights into purine metabolism in metabolic diseases: role of xanthine oxidoreductase activity. Am. J. Physiol. Endocrinol. Metabol. 319, E827–E834. https://doi.org/10.1152/ajpendo.00378.2020.

Garrido, P., Morán, J., García, A., González, S., González, C., 2013. 17 beta-estradiol activates glucose uptake via GLUT4 translocation and PI3K/akt signaling pathway in MCF-7 cells. Endocrinology 154. https://doi.org/10.1210/en.2012-1558.

Hernández-López, R., Torrens-Mas, M., Pons, D.G., Company, M.M., Falcó, E., Fernández, T., Ibarra de la Rosa, J.M., Roca, P., Oliver, J., Sastre-Serra, J., 2022. Mitochondrial function differences between tumor tissue of human metastatic and premetastatic CRC. Biology (Basel) 11. https://doi.org/10.3390/biology11020293.

Liu, L., Zhao, T., Shan, L., Cao, L., Zhu, X., Xue, Y., 2021. Estradiol regulates intestinal ABCG2 to promote urate excretion via the PI3K/Akt pathway. Nutr Metab (Lond) 18, 63. https://doi.org/10.1186/s12986-021-00583-y.

Ma, X., Wang, B., Guo, H., Zhang, Y., Zhu, G., Duan, Y., Yang, J., Zhang, D., Jin, L., Zhang, R., et al., 2010. [Tolerability of 6-mercaptopurine in children with acute lymphoblastic leukemia]. Zhonghua Er Ke Za Zhi 48, 289–292.

Maiuolo, J., Oppedisano, F., Gratteri, S., Muscoli, C., Mollace, V., 2016. Regulation of uric acid metabolism and excretion. Int. J. Cardiol. 213, 8–14. https://doi.org/10.1016/j.ijcard.2015.08.109.

Nielsen, O.H., Vainer, B., Rask-Madsen, J., 2001. Review article: the treatment of inflammatory bowel disease with 6-mercaptopurine or azathioprine. Aliment. Pharmacol. Ther. 15, 1699–1708. https://doi.org/10.1046/j.1365-2036.2001.01102.x.

Nishino, T., Okamoto, K., 2015. Mechanistic insights into xanthine oxidoreductase from development studies of candidate drugs to treat hyperuricemia and gout. JBIC, J. Biol. Inorg. Chem. 20, 195–207. https://doi.org/10.1007/s00775-014-1210-x.

Pedley, A.M., Benkovic, S.J., 2017. A new view into the regulation of purine metabolism: the purinosome. Trends Biochem. Sci. 42, 141–154. https://doi.org/10.1016/j.tibs.2016.09.009.

Saitoh, M., Nagai, K., Nakagawa, K., Yamamura, T., Yamamoto, S., Nishizaki, T., 2004. Adenosine induces apoptosis in the human gastric cancer cells via an intrinsic pathway relevant to activation of AMP-activated protein Kinase. Biochem. Pharmacol. 67, 2005–2011. https://doi.org/10.1016/j.bcp.2004.01.020.

Sasso, C., Santiano, F., Campo Verde Arbocco, F., Zyla, L., Semino, S., Guerrero-Gimenez, M., Creydt, V., López-Fontana, C., Carón, R., 2019. Estradiol and progesterone regulate proliferation and apoptosis in colon cancer. Endocr Connect 8. https://doi.org/10.1530/EC-18-0374.

Wada-Hiraike, O., Imamov, O., Hiraike, H., Hultenby, K., Schwend, T., Omoto, Y., Warner, M., Gustafsson, J.-Å., 2006. Role of estrogen receptor β in colonic epithelium. Proc. Natl. Acad. Sci. USA 103, 2959–2964. https://doi.org/10.1073/pnas.0511271103.

Wang, Y., Charchar, F.J., 2021. Establishment of sex difference in circulating uric acid is associated with higher testosterone and lower sex hormone-binding globulin in adolescent boys. Sci. Rep. 11, 17323. https://doi.org/10.1038/s41598-021-96959-4.

Xi, Y., Xu, P., 2021. Global colorectal cancer burden in 2020 and projections to 2040. Transl. Oncol. 14, 101174. https://doi.org/10.1016/j.tranon.2021.101174.

Yin, J., Ren, W., Huang, X., Deng, J., Li, T., Yin, Y., 2018a. Potential mechanisms connecting purine metabolism and cancer therapy. Front. Immunol. 9, 1697. https://doi.org/10.3389/fimmu.2018.01697.

Yin, J., Ren, W., Huang, X., Deng, J., Li, T., Yin, Y., 2018b. Potential mechanisms connecting purine metabolism and cancer therapy. Front. Immunol. 9, 1697. https://doi.org/10.3389/fimmu.2018.01697.